

Link Topology and Multi-Objective Mission Flow Optimization for Remote Sensing Satellites with Inter-Layer Links and Satellite-Ground Links

Xiaoqing Zhong, Ningxuan Guo, Yuqi Wang, Anshou Li, Liang Liu, Yupeng Gong, and Ningyuan Wang

Abstract—In the future Space Information Network (SIN), remote sensing satellites (RSSs) can access communication constellations (CC) and ground stations (GSs) through inter-layer links (ILLs) and satellite-ground links (SGLs) to realize the timely transmission of large amounts of observation data. In this paper, we study the link topology of both ILLs and SGLs with different time slot durations from the perspective of each RSS based on the time-expanded graph. We propose a multi-objective mission flow optimization model to jointly achieve transmission benefits maximization, end-of-period energy maximization, and transmission wait time minimization. This model considers missions' importance differences under limited storage, energy, and link bandwidth resources. To reduce the solving complexity, we propose a Phased Multi-Objective (PMO) algorithm composed of two Integer Linear Programming (ILP) problems and one Linear Programming (LP) problem to separate the integer programming part from the continuous part. A Multi-Objective Mixed Integer Linear Programming (MO-MILP) model is also formulated for comparison. We simulate the proposed methods in different scale SIN with practical parameters referred to the SAR satellites. The results indicate that observation data can be transmitted in near real-time with adequate bandwidth of ILLs. PMO can achieve multiple objectives and is applicable in large-scale constellation systems.

Index Terms—remote sensing satellites, space information network, inter-layer and satellite-ground links, time-expanded graph, multi-objective mission flow optimization.

I. INTRODUCTION

Earth observation of remote sensing satellites (RSSs) plays an important role in environmental monitoring, disaster emergency rescue, and smart city construction [1], [2]. With the development of RSSs, high-resolution and wide-range imaging results in a rapid increase of observation data amount. However, the traditional RSS system can only transmit data in

the visible range of ground stations (GSs) by satellite-ground links (SGLs). Due to political factors, GSs can only be placed in a small area (i.e. within the national territory), so RSSs have to transmit data at long intervals. As a result, it increases the onboard storage pressure of RSS and is unable to meet the needs of some real-time services.

Fortunately, communication constellation (CC) provides the possibility to realize the timely transmission of large amounts of observation data. In recent years, mega CC such as OneWeb [3], Starlink [4], Telesat [5] etc., have attracted much attention. They can transmit data back to earth at any time with the support of inter-satellite laser communications [6]. Hundreds of RSSs can access CC concurrently by inter-layer links (ILLs) to transmit observation data. These satellites and GSs form a Space Information Network (SIN) with a larger degree of connectivity [7]–[10]. Meanwhile, RSSs are also facing many changes in the design of satellite systems, such as a laser communication device mounted on the top or side of the satellite, a storage and energy system considering data transmission of ILLs, etc. For effectively transmitting data of RSSs in the SIN, it is crucial to study the SGLs and ILLs planning problem considering the highly dynamic characteristics of space topology, and the data flow optimization problem considering the onboard storage and energy resources. On this issue, research efforts have been undertaken in two aspects.

One aspect focuses on the dynamic time-varying space topology and link allocation strategy of the SIN. In this aspect, snapshot graph (or virtual topology) method is widely applied to divide the time domain evenly into several segments and name each segment as a time slot [11], [12]. The topology of each time slot is considered static, which means the visible relationships among all nodes are constant during a time slot. Hou et al. [13] proposed an SGLs planning algorithm to realize the minimum number of handover times and route updates. Li et al. [14] developed a time-relevant graph with time-domain and spatial-domain in a triple-layered satellite network, and proposed a topology control method. Huang et al. [15] studied the ILLs allocation strategy in a double-layered satellite network, with the consideration of satellites' visible duration, transmitting power, and distributions of user load.

However, the above-mentioned researches [13]–[15] only focus on the topology but do not reflect the optimization of data flow. Besides, the link allocation strategies do not consider the requirements of missions. Since flow planning is necessary for RSSs' data transmission, our research focuses on the other aspect as below.

This work was supported in part by the 173 Plan Domain Foundation under Grant 2023-JCJQ-JJ-0491, and in part by the National Natural Science Foundation of China under Grant 62201371. (Corresponding author: Ningxuan Guo.)

Xiaoqing Zhong is with the Institute of Telecommunication and Navigation Satellites, China Academy of Space Technology, Beijing 100094, China, and also with the Department of Strategic and Advanced Interdisciplinary Research, Peng Cheng Laboratory, Shenzhen, Guangdong 518055, China (e-mail: hitzxq@126.com).

Ningxuan Guo, Anshou Li, and Yupeng Gong are with the Department of Strategic and Advanced Interdisciplinary Research, Peng Cheng Laboratory, Shenzhen, Guangdong 518055, China (e-mail: gnx@zju.edu.cn; liash@pcl.ac.cn; gyphit@163.com).

Yuqi Wang, Liang Liu, and Ningyuan Wang are with the Institute of Telecommunication and Navigation Satellites, China Academy of Space Technology, Beijing 100094, China (e-mail: wangyuqi_its@163.com; liuliang1945@buaa.edu.cn; ningyuan.wang@foxmail.com).

The other aspect focuses on link topology and further considers flow optimization. In this aspect, time-expanded graph is commonly used to model the network topology. Compared to typical snapshot graphs, the time-expanded graphs further consider data storage as a caching link to connect adjacent snapshots [16], [17]. Liu et al. [18] proposed a maximum flow routing strategy in SIN with a dynamic time slot duration determination model. Zhou et al. [19] considered mission difference and proposed a network benefits maximization method in terms of sum weighted transmitted data volume. Yan et al. [20] optimized the ILLs' topology in global navigation satellite systems to achieve the maximum throughput, and further in [21] optimized both ILLs and SGLs to minimize the average delay of data delivery from satellites to GSs.

However, these researches [18]–[21] still have some unsolved problems as follows:

- 1) SGLs and ILLs are not jointly planned with the consideration of their different connectable conditions from the perspective of RSSs. The challenge lies in the fact that ILLs require a long time slot duration to implement the linear modeling of laser link handover constraints [22], while SGLs require a short time slot duration to achieve the maximum linking duration in the short visible time window.
- 2) Single-objective optimization of data flow loses the achievement for other related objectives. Transmission benefits maximization, throughput maximization, delay minimization, harvest energy maximization, etc., are all vital objectives. How to realize the optimization of multiple objectives?
- 3) When jointly planning SGLs and ILLs, the traditional Mixed Integer Linear Programming (MILP) models could not realize the optimization of each mission flow due to the computational complexity, and only the optimal total flow of all missions can be achieved. The challenge lies in reducing complexity to optimize each data flow with dynamic links and enable the method to be applicable in large-scale SIN.

In this paper, we study the linking strategy and mission flow optimization method from the perspective of each RSS in the scenario of RSSs accessing CC and GSs. The link topology of RSS in SIN is based on the time-expanded graph. The observation missions' importance difference is comprehensively considered in links planning and flow management to realize multiple objectives. The onboard storage, energy, and linking loads resources are limited for each RSS, so resource management is also involved. With the proposed model, each mission flows through SGLs and ILLs can be planned optimally. We verify the effectiveness of the proposed method in SIN with five GSs and three constellations of 36, 136, and 500 satellites. The simulation parameters of RSSs refer to the real data of a SAR satellite.

Compared to the state of the art, the main contributions of this paper can be summarized as follows:

- A joint topology optimization model of SGLs and ILLs from the perspective of RSSs in a time-expanded graph containing CC and GSs, in which each type of link has

its own appropriate time slot duration.

- A multi-objective mission flow optimization model achieving the transmission benefits maximization, the end-of-period energy maximization and the mission-weighted transmission wait time minimization, with a linear weighting method to realize the primary goal of benefits maximization.
- A Phased Multi-Objective (PMO) algorithm composed of two Integer Linear Programming (ILP) problems and one Linear Programming (LP) problem to reduce complexity by separating the integer programming part from the continuous programming part, which can significantly reduce the solution time and obtain an optimal solution close to the global optimum of the Multi-Objective MILP (MO-MILP) algorithm.

The rest of this paper is organized as follows. Section II presents the system architecture of SIN and its time-expanded graph. The topology optimization models of SGLs and ILLs are formulated in Section III. Based on the obtained link topology, we propose a multi-objective model in Section IV to realize flow optimization of each mission and resource management. In Section V, a weight selection strategy is proposed for the multi-objective problem, a PMO algorithm is proposed to solve the link planning and flow optimization problem, and an integrated MO-MILP model is formulated for comparison. Section VI verifies the effectiveness of the proposed models and algorithms with the simulation in an SIN composed of varying number of satellites and five GSs. At last, Section VII concludes this paper and discusses the future work.

II. SYSTEM ARCHITECTURE

In this section, we introduce the architecture of the SIN first. Then, a time-expanded graph is defined for the link topology in SIN.

A. Space Information Network

Fig. 1 shows the architecture of SIN with two layers of Low Earth Orbit (LEO) satellites. These two layers are composed of two types of satellites. One type is mainly used for communications, and these satellites can form a CC. The other type is RSS which can generate lots of observation data. Each RSS can access CC or GSs with ILLs or SGLs for observation data transmission.

In this paper, we optimize data transmission from the perspective of each RSS. There are two kinds of data transmission paths as shown in Fig. 1:

- RSS numbered ① transmits data back to GSs with the help of intra-layer links in CC. This transmission path executes only when the RSS is out of the visible range of all GSs.
- RSS numbered ② directly transmits data to GSs through SGLs within the visible range of any GSs.

Although the routing strategy within CC affects the global transmission performance and efficiency, it is difficult for RSSs to consider the routing of CC due to the limited CC information available to RSSs and the extra costs for calculation,

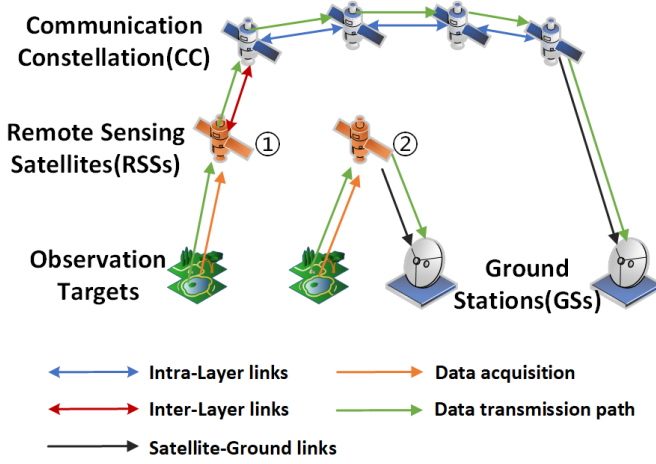


Fig. 1. Architecture of the Space Information Network.

communication, and storage. Considering the fact that RSSs and CC are not completely interoperable, we let RSSs only optimize their data transmission to CC or GSs and do not consider the routing strategy within CC in this paper. That is, we focus on ILLs and SGLs planning for RSSs, aiming to choose proper CC satellites or GSs to establish links and arrange mission flows optimally with limited resources.

B. Time-Expanded Graph

The link topology from RSSs to CC and GSs is denoted as a time-expanded graph, as shown in Fig. 2. Data storage links of graph nodes are shown as vertical purple lines in the figure. These storage links do not exist in practical systems, and the concept is introduced to represent the variation of data volume in memory between adjacent time slots. In this paper, since we optimize the inter-layer data transmission from the perspective of RSSs, we only consider the RSSs' data storage links and limited memory.

In the time-expanded graph, we use vertices to represent satellites, observation targets, and GSs. We use edges to represent the visible and linking relationships between RSS vertices and other vertices. We consider the duration of time slots can be different for ILLs' topology and SGLs' topology, which are $\Delta\tau_c$ and $\Delta\tau_g$, respectively. Generally, $\Delta\tau_c$ is larger than $\Delta\tau_g$, as shown in Fig. 2. Because the relative positions of a satellite and GSs are relatively fixed in each orbital period, they can connect as soon as they are in the visible range. Since we generally expect the satellite to be connected to GSs for the maximum potential duration in the short visible window, a short duration for SGLs' topology is appropriate. However, a relatively large time slot is needed for ILLs to reduce the complexity of the inter-layer irregular dynamic topology. Besides, a long time slot duration equal to the link handover interval can realize the linear modeling of laser link handover constraints [22].

As shown in Fig. 2, we should first evaluate the visible relationships of node pairs to obtain the potential links between each RSS and CC satellites or GSs. Then, we can decide on SGLs and ILLs for each RSS according to some optimal

TABLE I
DEFINITIONS OF NOTATIONS IN THE TIME-EXPANDED GRAPH

Notations	Definitions
$\mathcal{G}(\mathcal{V}, \mathcal{E})$	The time-expanded graph with vertices set \mathcal{V} and edges set \mathcal{E} .
$\mathcal{T}^c, T_c, \Delta\tau_c$	Set and number of time slots, duration of each time slot for ILLs.
$\mathcal{T}^g, T_g, \Delta\tau_g$	Set and number of time slots, duration of each time slot for SGLs.
i, j, k, t, f	Index of RSSs, CC satellites, GSs, time slots, and observation missions.
N_r, N_c, N_g, F_i	Number of RSSs, CC satellites, GSs, observation missions of RSS i .
$\mathcal{V}_t^o, \mathcal{V}_t^r, \mathcal{V}_t^c, \mathcal{V}_t^g$	Vertices set of observation targets, RSSs, CC satellites, and GSs at each time slot.
$\mathcal{E}_t^{or}, \mathcal{E}_t^{rc}, \mathcal{E}_t^{rg}, \mathcal{E}_t^{rs}$	Edges set of data acquisition, ILLs, SGLs, data storage of RSSs.
$\mathcal{F}_i, \mathbf{t}_i^s(f), \mathbf{t}_i^e(f), \mathbf{h}_i(f), \boldsymbol{\omega}_i(f)$	Observation mission set of RSS i , start time, end time, duration, importance factor of mission f .

linking rules. Note that if there are potential SGLs and ILLs in the same time slot, SGLs are selected with no doubt. But if the planned SGLs can not fulfill the whole time slot of $\Delta\tau_c$, ILLs would also be established in this time slot for seamless communication coverage, which is shown in $(\Delta\tau_c, 2\Delta\tau_c)$ horizon of links planning in Fig. 2. With the established links, the data flow of different missions can be arranged optimally with the limited link, storage, and energy resources under a unified time slot set. Each data flow starts from its observation target node, then goes to RSS through a data acquisition link, then it has three following choices: 1) passes to CC through ILLs; 2) passes to GSs through SGLs; 3) temporarily stored in the RSS and passes to subsequent time slot with the data storage links.

TABLE I lists the definition of notations in the time-expanded graph, their descriptions are as follows:

The graph $\mathcal{G} = \{\mathcal{V}, \mathcal{E}\}$, where \mathcal{V} and \mathcal{E} are the set of vertices and edges, respectively. Time slots set $\mathcal{T}^c = \{1, 2, \dots, T_c\}$ and $\mathcal{T}^g = \{1, 2, \dots, T_g\}$ for ILLs and SGLs, respectively. Define t as the index of each time slot.

Vertices set $\mathcal{V} = \{\mathcal{V}_t^o \cup \mathcal{V}_t^r \cup \mathcal{V}_t^c \cup \mathcal{V}_t^g | t \in \mathcal{T}^c \cup \mathcal{T}^g\}$, where the four components represent the observation targets nodes \mathcal{V}_t^o , the RSSs nodes $\mathcal{V}_t^r = \{i | i \in [1, N_r]\}$, the CC satellites nodes $\mathcal{V}_t^c = \{j | j \in [1, N_c]\}$, and the GSs nodes $\mathcal{V}_t^g = \{k | k \in [1, N_g]\}$, respectively.

Edges set $\mathcal{E} = \{\mathcal{E}_t^{or} \cup \mathcal{E}_t^{rc} \cup \mathcal{E}_t^{rg} \cup \mathcal{E}_t^{rs} | t \in \mathcal{T}^c \cup \mathcal{T}^g\}$, where \mathcal{E}_t^{or} represents data acquisition links, $\mathcal{E}_t^{rc} = \{(i, j) | i \in \mathcal{V}_t^r, j \in \mathcal{V}_t^c, t \in \mathcal{T}^c\}$ represents ILLs, $\mathcal{E}_t^{rg} = \{(i, k) | i \in \mathcal{V}_t^r, k \in \mathcal{V}_t^g, t \in \mathcal{T}^g\}$ represents SGLs, and $\mathcal{E}_t^{rs} = \{(i', i) | i' \in \mathcal{V}_{t-1}^r, i \in \mathcal{V}_t^r\}$ represents RSSs' data storage links.

Observation mission set $\mathcal{F}_i = \{f | f \in [1, F_i]\}$ for RSS i . Each mission f has characteristics $\{\mathbf{t}_i^s(f), \mathbf{t}_i^e(f), \mathbf{h}_i(f), \boldsymbol{\omega}_i(f)\}$, where $\mathbf{t}_i^s(f)$, $\mathbf{t}_i^e(f)$, and $\mathbf{h}_i(f)$ are the start time, end time and duration of data acquisition, $\boldsymbol{\omega}_i(f)$ is the importance factor. In this paper, we set the importance factor in the interval $[1, 10]$ and consider the observation missions are already arranged with specific execution time.

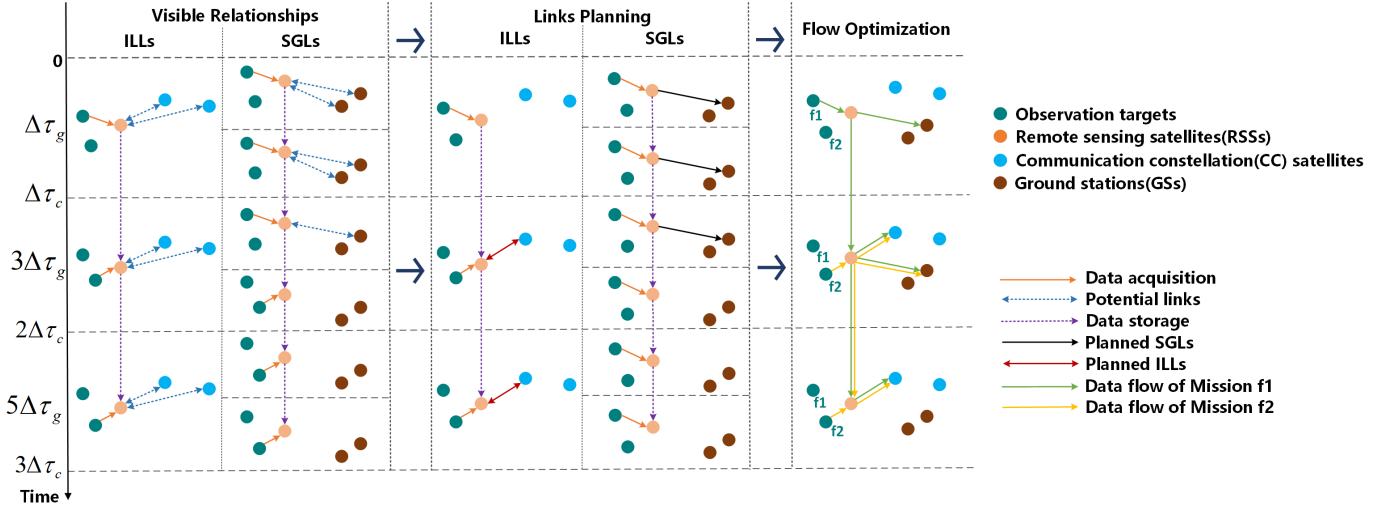


Fig. 2. Time-expanded graph of three stages: visible relationships, links planning, and flow optimization. The time slot duration of SGLs and ILLs is different. Here take $\Delta\tau_c = 2\Delta\tau_g$ as an example.

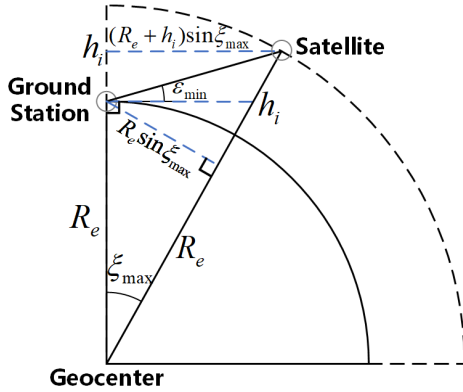


Fig. 3. Visible relationships between a satellite and a GS.

III. TOPOLOGY OPTIMIZATION MODEL

In this section, we formulate the links planning optimization problems of SGLs and ILLs to obtain the links planning graph.

A. Satellite-Ground Links Planning

1) *Visible Constraints*: As shown in Fig. 3, when a satellite and a GS are visible to each other, the GS should be in the coverage area of the satellite. When the GS is at the edge of the coverage area, the elevation angle is the minimum, defined as ε_{\min} . At this point, the geocentric angle between the satellite and the GS achieves the maximum ξ_{\max} as:

$$\xi_{\max} = \arccos\left(\frac{R_e}{R_e + a_i} \cos \varepsilon_{\min}\right) - \varepsilon_{\min} \quad (1)$$

where R_e is the Earth radius, a_i is the RSS's orbital altitude.

When the geocentric angle between RSS i and GS k is less than the maximum value ξ_{\max} , they are visible to each other. Define $\xi_i(k, t)$ be the geocentric angle between RSS i and GS k at time slot t . Let matrix $\mathbf{S}_i^g = \{\mathbf{S}_i^g(k, t) | k \in \mathcal{V}_t^g, t \in \mathcal{T}^g\} \in \mathbb{R}^{N_g \times T_g}$ represents the visible relationships of RSS i to all GSs at all time slots, which element $\mathbf{S}_i^g(k, t)$ is '1' when

RSS i and GS k are visible at time slot t , and '0' the opposite. Then, the visible matrix can be calculated by:

$$\mathbf{S}_i^g(k, t) = \begin{cases} 1, & \xi_i(k, t) \leq \xi_{\max} \\ 0, & \xi_i(k, t) > \xi_{\max} \end{cases} \quad \forall k \in \mathcal{V}_t^g, \forall t \in \mathcal{T}^g \quad (2)$$

Define $\delta_i^g = \{\delta_i^g(k, t) | k \in \mathcal{V}_t^g, t \in \mathcal{T}^g\} \in \mathbb{R}^{N_g \times T_g}$ be the decision matrix of SGLs, which element $\delta_i^g(k, t)$ is '1' when RSS i determine to establish an SGL with GS k at time slot t , and '0' the opposite. The value range of the decision variables satisfies:

$$\delta_i^g(k, t) \in \{0, 1\} \quad \forall k \in \mathcal{V}_t^g, \forall t \in \mathcal{T}^g \quad (3)$$

Then, the visible constraint can be described as:

$$\delta_i^g \leq \mathbf{S}_i^g \quad (4)$$

2) *Link Number Constraints*: We assume each RSS can only connect to one GS at each time slot, which means there is at most one SGL for an RSS at a time slot. The constraint can be described as:

$$\sum_{k \in \mathcal{V}_t^g} \delta_i^g(k, t) \leq 1 \quad \forall t \in \mathcal{T}^g \quad (5)$$

3) *SGLs Objective Formulation*: As for each RSS, we want the mission-weighted SGL benefits can be the maximum. It can help the satellite transmit data to GSs when executing important missions. Define $\omega_i(t)$ be the linking benefit at t time slot, it can be calculated by the mission importance factor $\omega_i(f)$ as follows:

$$\omega_i(t) = \begin{cases} \omega_i(f), & t \in \{[t_i^s(f), t_i^e(f)] | \forall f \in \mathcal{F}_i\} \\ 1, & \text{Others} \end{cases} \quad (6)$$

It means that when RSS i is executing observing missions, the linking benefit at this time slot is equal to the mission importance factor; while RSS i is not executing any missions, the linking benefit at this time slot is set to 1 (equals to the minimum mission importance factor).

Then, the objective can be formulated as:

$$y_1^g = \frac{\sum_{t \in \mathcal{T}^g} \left(\omega_i(t) \sum_{k \in \mathcal{V}_t^g} \delta_i^g(k, t) \right)}{\sum_{t \in \mathcal{T}^g} \left(\omega_i(t) \cdot \min \left\{ 1, \sum_{k \in \mathcal{V}_t^g} S_i^g(k, t) \right\} \right)} \quad (7)$$

where the numerator obtains the determined mission-weighted SGL benefits, and the denominator obtains the maximum benefits of potential SGLs. In the equation, $\min \left\{ 1, \sum_{k \in \mathcal{V}_t^g} S_i^g(k, t) \right\}$ can mark the time slot when the satellite is visible to at least one GS. The denominator means that when all visible time slots can establish SGLs, the linking benefits can achieve the maximum value. The denominator is used for normalization.

However, a satellite can be visible to several GSs in the same time slot, but (7) only considers SGLs in the time domain. Therefore, the SGLs solution may be non-unique, since connecting with different GSs at a certain time slot does not affect the value of y_1^g . So we add an item to obtain the unique solution by making the distance of SGLs as small as possible:

$$y_2^g = \frac{\sum_{t \in \mathcal{T}^g} \sum_{k \in \mathcal{V}_t^g} [\delta_i^g(k, t) (d_{\max}^g - d_i^g(k, t))]}{\sum_{t \in \mathcal{T}^g} \max \{ d_{\max}^g - d_i^g(k, t) S_i^g(k, t) | k \in \mathcal{V}_t^g \}} \quad (8)$$

where $d_i^g = \{d_i^g(k, t) | k \in \mathcal{V}_t^g, t \in \mathcal{T}^g\} \in \mathbb{R}^{N_g \times T_g}$ is the distance matrix between i and all GSs at all time slots, d_{\max}^g is the maximum distance of visible SGLs, and can be calculated by:

$$d_{\max}^g = \max \{ d_i^g(k, t) S_i^g(k, t) | k \in \mathcal{V}_t^g, t \in \mathcal{T}^g \} \quad (9)$$

In equation (8), d_{\max}^g is used to convert the minimum distance objective into a maximization form. In the denominator, $\max \{ d_{\max}^g - d_i^g(k, t) S_i^g(k, t) | k \in \mathcal{V}_t^g \}$ can mark the closest visible GSs at each time slot. Here, the denominator is also used for normalization.

Consequently, the SGLs planning objective function for each RSS can be formulated as:

$$\max_{\delta_i^g} \alpha_1 y_1^g + \alpha_2 y_2^g \quad \forall i \in \cup_{t \in \mathcal{T}^g} \mathcal{V}_t^r \quad (10)$$

subject to:

$$(1) \sim (9)$$

where α_1 and α_2 are weights of benefits and link distances.

Theorem 1. *The objective function (10) can realize the maximization of linking benefits with the minimized distances of SGLs by selecting any positive objective weight values of α_1 and α_2 .*

Proof. In (10), we hope to give the linking benefits y_1^g a higher priority. That is, when the objective function value already achieves the maximum benefits, we further select GSs with shorter distances.

Therefore, for a certain time slot t , consider two cases:

- Case 1: RSS i does not establish any SGLs at t .
- Case 2: RSS i establishes an SGL with the farthest GS at t , the distance $d_i^g(k, t) \leq d_{\max}^g$.

We consider Case 2 to be better because it can achieve a larger benefits value. Therefore, the objective value of this time slot t in Case 2 should be larger than Case 1, that is:

$$\alpha_1 \frac{\omega_i(t)}{y_1^g \text{ denominator}} + \alpha_2 \frac{(d_{\max}^g - d_i^g(k, t))}{y_2^g \text{ denominator}} > 0 \quad (11)$$

where the left side of the inequality is the objective value of this time slot in Case 2, and the right side '0' is the objective value of this time slot in Case 1.

Since (11) is always true, α_1 and α_2 can be any positive values. \square

Due to the denominators of (7), (8) and the calculation of d_{\max}^g in (9) are only related to known parameters S_i^g and d_i^g , the optimization of SGLs planning is formulated as an ILP model with $N_g \cdot T_g$ integer decision variables. The obtained non-zero elements in δ_i^g form the edges set \mathcal{E}_t^{rg} for all $t \in \mathcal{T}^g$.

4) *SGLs' Windows:* With the optimal linking variable δ_i^g , we can obtain the SGLs' windows. A duration in $\delta_i^g(k, :)$ with continuous '1' for a certain k is considered as an SGL window. Let $\mathbf{t}^{gs} \in \mathbb{R}^{N_w}$, $\mathbf{t}^{ge} \in \mathbb{R}^{N_w}$ denote the vector of the windows' start time and end time, where N_w is the number of windows. Then each element in \mathbf{t}^{gs} and \mathbf{t}^{ge} are the index of the first and last non-zero element of each window. Since we consider the SGLs preferentially, there is no need to arrange ILLs during the SGLs' windows. However, as introduced before, the duration of time slots are different for SGLs and ILLs, which are $\Delta\tau_g$ and $\Delta\tau_c$, respectively. For the convenience of ILLs planning, we need to transform SGLs' windows expressed in \mathcal{T}^g into the ILLs' time slot set \mathcal{T}^c . The time-transforming expression is:

$$\gamma = \frac{\Delta\tau_c}{\Delta\tau_g} \quad (12)$$

$$\mathbf{t}^{gs'} = \left\lceil \frac{\mathbf{t}^{gs}}{\gamma} \right\rceil + 1 \quad (13)$$

$$\mathbf{t}^{ge'} = \left\lfloor \frac{\mathbf{t}^{ge}}{\gamma} \right\rfloor \quad (14)$$

where $\mathbf{t}^{gs'} \in \mathbb{R}^{N_w}$, $\mathbf{t}^{ge'} \in \mathbb{R}^{N_w}$ are SGLs' windows expressed in \mathcal{T}^c , and $\lceil \cdot \rceil$ is the round up operation, $\lfloor \cdot \rfloor$ is the round down operation.

With the transforming expressions (13) and (14), SGLs and ILLs can be overlapped in a short duration to achieve the seamless handover of SGLs and ILLs. Note that γ should be an integer, so we need to make sure that $\Delta\tau_c$ is divisible by $\Delta\tau_g$.

B. Inter-Layer Links Planning

1) *Definition and Windows' Constraints:* Define $\delta_i^c = \{\delta_i^c(j, t) | j \in \mathcal{V}_t^c, t \in \mathcal{T}^c\} \in \mathbb{R}^{N_c \times T_c}$ be the decision matrix of ILLs for RSS i to all CC satellites at all time slots. Since we do not need to arrange ILLs when there are SGLs, we need to

constrain $\delta_i^c(j, t)$ to zero in the SGLs' transformed windows. The constraints can be described as:

$$\delta_i^c(j, t) = 0 \quad \forall j \in \mathcal{V}_t^c, \forall t \in [\mathbf{t}^{gs'}, \mathbf{t}^{ge'}] \quad (15)$$

$$\delta_i^c(j, t) \in \{0, 1\} \quad \forall j \in \mathcal{V}_t^c, \forall t \in \mathcal{T}^c \quad (16)$$

2) *ILLs Objective Formulation*: The ILLs planning objective is to maximize the mission-weighted ILLs benefits. The objective function can be formulated as follows:

$$\max_{\delta_i^c} \sum_{t \in \mathcal{T}^c} \left(\omega_i(t) \sum_{j \in \mathcal{V}_t^c} \delta_i^c(j, t) \right) \quad (17)$$

subject to:

$$(15) \sim (16)$$

$$\delta_i^c \leq \mathbf{S}_i^c \quad (18)$$

$$\sum_{j \in \mathcal{V}_t^c} \delta_i^c(j, t) \leq 1 \quad \forall t \in \mathcal{T}^c \quad (19)$$

$$|\delta_i^c(:, t) - \delta_i^c(:, t-1)| \leq 1 \quad \forall t \in [2, T_c] \quad (20)$$

$$|\delta_i^c(:, t) - \delta_{i,0}^c| \leq 1 \quad t = 1 \quad (21)$$

where $\mathbf{S}_i^c = \{\mathbf{S}_i^c(j, t) | j \in \mathcal{V}_t^c, t \in \mathcal{T}^c\} \in \mathbb{R}^{N_c \times T_c}$ is the connectable relationship matrix and can be obtained according to the authors' previous work in [22], $\delta_{i,0}^c = \{\delta_{i,0}^c(j) | j \in \mathcal{V}_t^c\} \in \mathbb{R}^{N_c}$ is the initial linking status vector from i to all CC satellites.

Inequality (18) constrains ILLs can be established only when the two satellites are connectable. Constraint (19) indicates an RSS can only establish one ILL at a time slot. Inequalities (20) and (21) are the norm constraints of vectors and can guarantee enough link handover time for ILLs since the recapture is essential for inter-satellite laser communications. The detail explanation of (20) and (21) can be found in the authors' previous work [22]. Note that the time slot duration $\Delta\tau_c$ needs to be longer than the necessary link handover duration.

Since the norm constraints (20) and (21) are linear, the optimization of ILLs planning is formulated as an ILP model with $N_c \cdot T_c$ integer decision variables. With the obtained non-zero elements in δ_i^c , the edges set \mathcal{E}_t^{rc} for all $t \in \mathcal{T}^c$ can be formed.

IV. MULTI-OBJECTIVE MODEL OF FLOW PLANNING AND RESOURCE MANAGEMENT

With the planned SGLs and ILLs, we can arrange data flow for each mission with the time-expanded graph. As for each RSS, the limited link, storage, and energy resources are taken into account.

A. Flow-related Constraints

Define $\mathbf{q}_i^g = \{\mathbf{q}_i^g(f, t) | f \in \mathcal{F}_i, t \in \mathcal{T}^g\} \in \mathbb{R}^{F_i \times T_g}$ (in Gbit) be the flow quantity matrix of all missions in all time slots with SGLs of RSS i . Let $\mathbf{q}_i^c = \{\mathbf{q}_i^c(f, t) | f \in \mathcal{F}_i, t \in \mathcal{T}^c\} \in \mathbb{R}^{F_i \times T_c}$ be the flow quantity matrix with ILLs. It can be noted that the linking objects $k \in \mathcal{V}_t^g$ or $j \in \mathcal{V}_t^c$ are not reflected in matrices \mathbf{q}_i^g and \mathbf{q}_i^c , this is because each RSS can only connect

to one GS and CC satellite at a time slot, so each time slot corresponds to a unique SGL or a unique ILL. Therefore, we only need to arrange missions in the time domain. The flow-related constraints are described as follows.

1) *Flow Range*: Define $\nu_i^{rg}(k)$ (in Gbit/s) be the transmission rate of SGL (i, k) , and $\nu_i^{rc}(j)$ be the transmission rate of ILL (i, j) . The flow quantity of all missions should not exceed the corresponding links' capacity, so the lower and upper bounds of flow variables can be described as:

$$\mathbf{q}_i^g(f, t) \geq 0 \quad \forall f \in \mathcal{F}_i, \forall t \in \mathcal{T}^g \quad (22)$$

$$\mathbf{q}_i^c(f, t) \geq 0 \quad \forall f \in \mathcal{F}_i, \forall t \in \mathcal{T}^c \quad (23)$$

$$\sum_{f \in \mathcal{F}_i} \mathbf{q}_i^g(f, t) \leq \sum_{k \in \mathcal{V}_t^g} (\delta_i^g(k, t) \cdot \nu_i^{rg}(k) \cdot \Delta\tau_g) \quad \forall t \in \mathcal{T}^g \quad (24)$$

$$\sum_{f \in \mathcal{F}_i} \mathbf{q}_i^c(f, t) \leq \sum_{j \in \mathcal{V}_t^c} (\delta_i^c(j, t) \cdot \nu_i^{rc}(j) \cdot \Delta\tau_c) \quad \forall t \in \mathcal{T}^c \quad (25)$$

where $\delta_i^g(k, t)$ and $\delta_i^c(j, t)$ in (24) and (25) let data only flow through planned ILLs and SGLs.

2) *Flow Balance and Storage Capacity*: Define $\mathbf{b}_i = \{\mathbf{b}_i(f, t) | f \in \mathcal{F}_i, t \in \mathcal{T}^c\} \in \mathbb{R}^{F_i \times T_c}$ (in Gbit) be the data volume matrix stored in RSS i 's memory of all missions at the end of all time slots. It can be calculated by (26), which is at the top of next page. Recall that $\mathbf{t}_i^s(f)$ and $\mathbf{t}_i^e(f)$ are the start and end time of data acquisition for each mission f , and γ is the ratio of $\Delta\tau_c$ and $\Delta\tau_g$, as expressed in (12). The data acquisition rate is ν_i^{or} . In the equation (26), the flow balance is followed for each mission. That is, the data volume of each mission f stored in memory at the end of each time slot equals the total obtained data quantity of f minus the total transmitted data quantity of f until the end of each time slot. The time slot set is unified into \mathcal{T}^c by multiplying t with γ when calculating the total transmitted data through SGLs.

The limited memory capacity constraints can be expressed as:

$$\mathbf{b}_i(f, t) \geq 0 \quad \forall f \in \mathcal{F}_i, \forall t \in \mathcal{T}^c \quad (27)$$

$$b_{i,0} + \sum_{f \in \mathcal{F}_i} \mathbf{b}_i(f, t) \leq b_i^{\max} \quad \forall t \in \mathcal{T}^c \quad (28)$$

where $b_{i,0}$ represents the initial data volume stored in memory. Inequalities (27) and (28) constrain the stored data volume to be non-negative and do not exceed the maximum memory capacity b_i^{\max} .

B. Energy-related Constraints

1) *Energy Harvesting*: RSSs can harvest energy by solar panels during sunlight periods. Define $\mathbf{E}_i^H = \{\mathbf{E}_i^H(t) | t \in \mathcal{T}^c\} \in \mathbb{R}^{T_c}$ be the harvested energy vector at all time slots. The harvested energy at each time slot should not exceed the maximum volume that can be collected during the sunlight duration of this time slot, which can be expressed as:

$$0 \leq \mathbf{E}_i^H(t) \leq P^H \cdot l_{i,t} \quad \forall t \in \mathcal{T}^c \quad (29)$$

where P^H is the output power of solar panels, $l_{i,t}$ is RSS i 's sunlight duration in time slot t , whose values belong to the interval $[0, \Delta\tau_c]$.

$$b_i(f, t) = \begin{cases} 0 & \forall t \in [1, \max\{1, t_i^s(f) - 1\}], \forall f \in \mathcal{F}_i \\ \nu_i^{or} \cdot \Delta\tau_c \cdot [t - t_i^s(f) + 1] - \left(\sum_{t=1}^t q_i^c(f, t) + \sum_{t=1}^{t \cdot \gamma} q_i^g(f, t) \right) & \forall t \in [t_i^s(f), t_i^e(f)], \forall f \in \mathcal{F}_i \\ \nu_i^{or} \cdot \Delta\tau_c \cdot h_i(f) - \left(\sum_{t=1}^t q_i^c(f, t) + \sum_{t=1}^{t \cdot \gamma} q_i^g(f, t) \right) & \forall t \in [t_i^e(f) + 1, T_c], \forall f \in \mathcal{F}_i \end{cases} \quad (26)$$

2) *Energy Consumption*: Define $\mathbf{E}_i^C = \{\mathbf{E}_i^C(t) | t \in \mathcal{T}^c\} \in \mathbb{R}^{T_c}$ be the consumed energy vector at all time slots. It is composed of three parts: observing mission energy consumption $\mathbf{E}_i^M(t)$, transmitting energy consumption $\mathbf{E}_i^S(t)$, and the other conventional operating energy consumption, which can be expressed as:

$$\mathbf{E}_i^C(t) = \mathbf{E}_i^M(t) + \mathbf{E}_i^S(t) + P^O \cdot \Delta\tau_c \quad \forall t \in \mathcal{T}^c \quad (30)$$

$$\mathbf{E}_i^M(t) = \begin{cases} P^M \cdot \Delta\tau_c, & t \in \{[t_i^s(f), t_i^e(f)] | \forall f \in \mathcal{F}_i\} \\ 0, & \text{Others} \end{cases} \quad (31)$$

$$\mathbf{E}_i^S(t) = \sum_{f \in \mathcal{F}_i} \left(\sum_{j \in \mathcal{V}_i^c} P^{Sc} \cdot \frac{\delta_i^c(j, t) \cdot q_i^c(f, t)}{\nu_i^{rc}(j)} + \sum_{(t-1)\gamma+1}^{t \cdot \gamma} \sum_{k \in \mathcal{V}_i^g} P^{Sg} \cdot \frac{\delta_i^g(k, t) \cdot q_i^g(f, t)}{\nu_i^{rg}(k)} \right) \quad (32)$$

where P^O is the operating power, P^M is the constant observing mission power, P^{Sc} and P^{Sg} are the transmitting power of ILLs and SGLs, respectively. Here, the time slot sets are also unified into \mathcal{T}^c by multiplying t with γ for SGLs' energy consumption.

3) *Onboard Energy Range*: Define $\mathbf{E}_i = \{\mathbf{E}_i(t) | t \in \mathcal{T}^c\} \in \mathbb{R}^{T_c}$ be the onboard energy vector at the end of all time slots. The value of $\mathbf{E}_i(t)$ is related to the initial energy $E_{i,0}$, the harvested energy $\mathbf{E}_i^H(t)$ and the consumed energy $\mathbf{E}_i^C(t)$ at each time slot as:

$$\mathbf{E}_i(t) = E_{i,0} + \sum_{t=1}^t \mathbf{E}_i^H(t) - \sum_{t=1}^t \mathbf{E}_i^C(t) \quad \forall t \in \mathcal{T}^c \quad (33)$$

where the onboard energy should not exceed the maximum battery capacity E_i^{\max} and the maximum discharge depth θ , which can be described as:

$$E_i^{\max}(1 - \theta) \leq \mathbf{E}_i(t) \leq E_i^{\max} \quad \forall t \in \mathcal{T}^c \quad (34)$$

C. Multi-Objective Formulation

1) *Maximizing the Mission-weighted Data Transmission Benefits*: The main objective of flow planning and resource management is to make data transmitted to CC or GSs as much as possible. Since different missions have different importance factors, we want important data can be transmitted with priority. The transmission benefits are defined as the sum of

mission-weighted data volumes that complete the transmission through SGLs or ILLs. This objective can be formulated as:

$$\max y_1 = \frac{\sum_{f \in \mathcal{F}_i} \left[\left(\sum_{t \in \mathcal{T}^c} q_i^c(f, t) + \sum_{t \in \mathcal{T}^g} q_i^g(f, t) \right) \omega_i(f) \right]}{\sum_{f \in \mathcal{F}_i} (\nu_i^{or} \cdot \Delta\tau_c \cdot h_i(f) \cdot \omega_i(f))} \quad (35)$$

where the denominator is used for normalization, which represents the maximum benefits that assume all generated mission data are transmitted.

2) *Maximizing the Onboard Energy at the end of the Planning Horizon*: Since the energy-related constraints (29)~(34) can only guarantee the onboard energy is enough for transmitting data in this planning horizon, the satellite's operation after the horizon is ignored. So even if more energy could be harvested, the satellite would not do the obvious "right" thing if the energy consumption had been satisfied during this horizon. But there may be a situation in which the current planning horizon has much time in the sunlight, while the next horizon will be mostly in the umbra. Therefore, for the long-term operation of the satellite, we want the onboard energy at the end of the planning horizon to be as much as possible. This objective can be formulated as:

$$\max y_2 = \frac{\mathbf{E}_i(T_c)}{E_i^{\max}} \quad (36)$$

where the numerator is the onboard energy at the end of T_c , and the denominator is the maximum energy capacity used for normalization.

3) *Minimizing the Mission-weighted Transmission Wait Time*: We hope the mission data can be transmitted as soon as possible to meet real-time business needs. We also consider the mission importance factor for the transmission wait time, so important data can be transmitted with a priority when the link resources are limited. The transmission wait time of f is the difference between the transmission completed time and $t_i^e(f)$. However, the transmission completed time is the larger index of the last non-zero element in $\mathbf{q}_i^c(f, :)$ and $\mathbf{q}_i^g(f, :)$, which is a nonlinear expression. To minimize wait time simply and linearly, we turn to the mission-weighted stored data volume in memory, since the stored data minimization means that all data need to avoid storage and be transmitted soon, especially those important mission data. Consequently, this objective can

be formulated as:

$$\min y_3 = \frac{\sum_{f \in \mathcal{F}_i} \left(\omega_i(f) \sum_{t \in \mathcal{T}^c} b_i(f, t) \right)}{\sum_{f \in \mathcal{F}_i} (\nu_i^{or} \cdot \Delta \tau_c \cdot \mathbf{h}_i(f) \cdot \omega_i(f))} \quad (37)$$

where the objective y_3 should be minimized. The numerator is the sum of the mission-weighted stored data in memory of all time slots. The denominator is the maximum mission-weighted stored data volume assuming all mission data is stored in memory.

V. SOLUTION APPROACH

In this section, we first introduce the linear weighting method to transform the multi-objective problem proposed in Section IV into a single-objective optimization problem. Secondly, we propose a phased solving algorithm to solve the proposed problems introduced in Section III and Section IV. Then, to verify the effectiveness of the proposed algorithm, we integrate the proposed models into an MILP model for comparison. Last but not least, we analyze the optimality and complexity of the proposed algorithm and the MILP problem.

A. Linear Weighting of the Multi-objective Problem

As introduced in Section IV, the objective of flow planning and resource management is to jointly maximize the data transmission benefits, maximize the onboard energy for later operation, and minimize the transmission wait time, with the consideration of the mission importance factor. We use the linear weighting method [23] to transform the three objective functions into a single-objective optimization problem as follows:

$$\max_{q_i^g, q_i^e, E_i^H} \beta_1 y_1 + \beta_2 y_2 - \beta_3 y_3 \quad \forall i \in \cup_{t \in \mathcal{T}^c} \mathcal{V}_t^r \quad (38)$$

subject to:

$$(22) \sim (37)$$

where β_1 , β_2 , and β_3 are the weight values of the three objectives.

The three objectives have conflicts with each other, because more benefits (larger value of y_1) result in more energy consumption (smaller value of y_2) and possibly longer transmission wait time (larger value of y_3). Therefore, the objective weights should be carefully selected. We consider the benefits should be optimized preferentially because the main goal of flow planning is to make more important data be transmitted.

Theorem 2. By selecting the following weights value (39), the optimization problem (38) can achieve the primary goal of benefits maximization (35), and secondary objectives of energy maximization (36) and wait time minimization (37).

$$\begin{cases} \beta_1 = \max \left\{ \frac{\theta \cdot \sum_{f \in \mathcal{F}_i} (\mathbf{h}_i(f) \omega_i(f))}{\min\{\mathbf{h}_i(f) | f \in \mathcal{F}_i\} \min\{\omega_i(f) | f \in \mathcal{F}_i\}}, T_c \right\} \\ \beta_2 = 1 \\ \beta_3 = 1 \end{cases} \quad (39)$$

Proof. (a) Relationship of β_1 and β_2 . For a certain mission f , considering two cases:

- Case 1: $\max y_1$ and $\min y_2$. So f is transmitted to obtain benefits, and the least energy has been harvested with $E_i(T_c) = E_i^{\max}(1 - \theta)$.
- Case 2: $\min y_1$ and $\max y_2$. So f is not transmitted, and the energy is harvested to the maximum $E_i(T_c) = E_i^{\max}$.

The two cases may have close results, but we hope the objective value $\beta_1 y_1 + \beta_2 y_2$ for this mission f in Case 1 is better than Case 2, because Case 1 can obtain more benefits. Therefore, the following inequality should be satisfied:

$$\beta_1 \frac{\nu_i^{or} \Delta \tau_c \mathbf{h}_i(f) \omega_i(f)}{\sum_{f \in \mathcal{F}_i} (\nu_i^{or} \Delta \tau_c \mathbf{h}_i(f) \omega_i(f))} + \beta_2 \cdot \frac{E_i^{\max}(1 - \theta)}{E_i^{\max}} > \beta_1 \cdot 0 + \beta_2 \frac{E_i^{\max}}{E_i^{\max}} \quad (40)$$

After simplification, we have:

$$\beta_1 > \frac{\theta \cdot \sum_{f \in \mathcal{F}_i} (\mathbf{h}_i(f) \omega_i(f))}{\mathbf{h}_i(f) \omega_i(f)} \beta_2 \quad (41)$$

Taking the maximum value of the right side, we can obtain:

$$\beta_1 \geq \frac{\theta \cdot \sum_{f \in \mathcal{F}_i} \mathbf{h}_i(f) \omega_i(f)}{\min\{\mathbf{h}_i(f) | f \in \mathcal{F}_i\} \min\{\omega_i(f) | f \in \mathcal{F}_i\}} \beta_2 \quad (42)$$

Then if (42) is satisfied, (41) must be satisfied.

(b) Relationship of β_1 and β_3 . For certain missions f and f' satisfying $\mathbf{h}_i(f) = \mathbf{h}_i(f')$ and $\omega_i(f) = \omega_i(f')$, considering two cases:

- Case 3: $\max y_1$ and $\max y_3$. So f is transmitted to obtain benefits but wait for the longest time (collected at the first $\mathbf{h}_i(f)$ time slots, transmitted at the last $\nu_i^{or} \mathbf{h}_i(f) / \nu_i^{rc}(j)$ time slots, assuming transmitted by ILLs).
- Case 4: $\min y_1$ and $\min y_3$. So f' is not transmitted, and the data is collected at the last $\mathbf{h}_i(f')$ time slots.

Transmitting data of f and f' can obtain the same benefits, so the two cases may have close results. We hope the objective value $\beta_1 y_1 - \beta_3 y_3$ for mission f in Case 3 is better than mission f' in Case 4, because Case 3 can obtain larger benefits. Therefore, the following inequality should be satisfied:

$$\frac{\mathbf{h}_i(f) \omega_i(f)}{\sum_{f \in \mathcal{F}_i} \mathbf{h}_i(f) \omega_i(f)} \left[\beta_1 - \beta_3 \left(T_c - \frac{\mathbf{h}_i(f) + 1}{2} - \frac{\nu_i^{or} \mathbf{h}_i(f)}{2\nu_i^{rc}(j)} \right) \right] > \beta_1 \cdot 0 - \beta_3 \frac{\mathbf{h}_i(f) \omega_i(f)}{\sum_{f \in \mathcal{F}_i} \mathbf{h}_i(f) \omega_i(f)} \cdot \frac{1 + \mathbf{h}_i(f)}{2} \quad (43)$$

After simplification, we have:

$$\beta_1 > \beta_3 \left(T_c - \mathbf{h}_i(f) - 1 - \frac{\nu_i^{or} \mathbf{h}_i(f)}{2\nu_i^{rc}(j)} \right) \quad (44)$$

Then if (45) is satisfied, (44) must be satisfied.

$$\beta_1 \geq T_c \beta_3 \quad (45)$$

Synthesize the relationships of β_1 , β_2 , and β_3 in (42) and (45), the value of weights in (39) can be obtained to achieve the primary goal of benefits maximization. \square

In the linear weighted optimization problem (38), variables are $q_i^g, q_i^c, b_i, E_i^H, E_i^C, E_i^S(t), E_i$, and known parameters are $\delta_i^g, \delta_i^c, \nu_i^{rg}(k), \nu_i^{rc}(j), \nu_i^{or}, \Delta\tau_g, \Delta\tau_c, b_{i,0}, b_i^{\max}, l_{i,t}, P^H, P^M, P^O, P^{Sc}, P^{Sg}, E_i^M(t), E_{i,0}, E_i^{\max}, \theta, \omega_i(f), t_i^s(f), t_i^e(f), h_i(f), F_i, T_c, T_g, N_c, N_g$.

Among variables, b_i, E_i^C and $E_i^S(t)$ are determined by q_i^g and q_i^c according to (26) and (30)~(32), and E_i is determined by E_i^H, q_i^g and q_i^c according to (33). Therefore, the decision variables are q_i^g, q_i^c and E_i^H in this optimization problem, as expressed in (38).

The optimization of flow planning and resource management is formulated as an LP model with $(F_i \cdot T_g + F_i \cdot T_c + T_c)$ decision variables. The obtained value $b_i(f, t) - b_i(f, t - 1)$ corresponds to the data quantity of each mission flow in the storage edges set \mathcal{E}_t^{rs} . The value of $q_i^g(f, t)$ and $q_i^c(f, t)$ correspond to the data quantity of each mission flow in link edges set \mathcal{E}_t^{rg} and \mathcal{E}_t^{rc} , respectively.

B. Phased Solving Algorithm

In this paper, we solve the SGLs planning problem, ILLs planning problem, and the linear weighted multi-objective flow planning problem sequentially. The solving process of the entire mission data transmission method is illustrated in Algorithm 1, named the Phased Multi-Objective (PMO) optimization algorithm.

Algorithm 1 PMO: a phased multi-objective mission data transmission optimization algorithm.

-
- 1: **for** each RSS $i \in \mathcal{V}_t^r$ **do**
 - 2: Plan SGLs δ_i^g by solving the ILP problem (10) subject to (1)~(9).
 - 3: With the obtained δ_i^g , calculate SGLs' windows t^{gs}, t^{ge} expressed in \mathcal{T}^g .
 - 4: Transform SGLs' windows to $t^{gs'}, t^{ge'}$ expressed in \mathcal{T}^c with (12)~(14).
 - 5: Plan ILLs δ_i^c by solving the ILP problem (17) subject to (15)~(16), (18)~(21).
 - 6: With the obtained SGLs δ_i^g and ILLs δ_i^c , optimize flow for each mission and manage storage and energy resources by solving the linear weighted multi-objective problem (38) subject to (22)~(37), (39).
 - 7: **end for**
-

Steps 2~5 solve SGLs and ILLs planning problems separately, whereas steps 3~4 connect the two problems through the SGLs' windows calculated by δ_i^g , to ensure that no ILLs are established in the SGLs' windows. Step 6 solves the linear weighted multi-objective problem to optimize data flow and resource allocation.

Note that the linking limits of CC satellites and GSs are not taken into account in this paper. Therefore, we plan SGLs and ILLs from the perspective of each RSS and consider the planned links as the final topology. If CC satellites and GSs have limited linking devices, we can add a distributed request and reply process between step 5 and step 6 refer to the authors' previous work in [22]. It means that each RSS requests corresponding objects for SGLs and ILLs, and each

CC satellite and each GS can reject some requests according to its linking limits. In this way, the final topology would be adjusted and confirmed by CC satellites and GSs.

C. Mixed Integer Linear Programming

As studied in many existing research [18]–[21], the links planning problem and the flow management problem can be modeled as a whole MILP optimization problem. In this paper, the proposed PMO has three optimization problems. They can be considered as being decomposed from a Multi-Objective MILP (MO-MILP) model as follows:

$$\max_{\delta_i^g, \delta_i^c, q_i^g, q_i^c, E_i^H} \beta_1 y_1 + \beta_2 y_2 - \beta_3 y_3 \quad (46)$$

subject to:

$$(1) \sim (5), (12) \sim (16), (18) \sim (37), (39)$$

where $\delta_i^g, \delta_i^c, q_i^g, q_i^c, E_i^H$ are decision variables.

Note that t^{gs} and t^{ge} in (13) and (14) here are the vector of SGLs' visible windows' start time and end time, respectively. They are generated from S_i^g instead of δ_i^g . It means that if an RSS has visible GSs, it will not establish ILLs during this time window. In this way, the priority of SGLs can be guaranteed.

The MO-MILP model can obtain the global optimum by jointly solving the SGLs planning, ILLs planning, and flow management problems.

D. Optimality Analysis

SGLs and ILLs planning problems are related to each other by constraints (13)~(15). In PMO, the variables t^{gs} and t^{ge} of SGLs' windows are calculated by the linking variables δ_i^g . Both SGLs and ILLs planning problems pursue covering more time slots with communication links. Therefore, when solving the SGLs planning problem, if there is a visible GS at a certain time slot, an SGL must be established at that time slot. Then, when solving the ILLs planning problem, the other time slots will be tried best to be covered by ILLs.

If we solve the SGLs and ILLs planning problems jointly, the variables t^{gs} and t^{ge} should be calculated by the visible matrix S_i^g . But this will not change the fact that SGLs be established at any time slots with visible GSs, and ILLs will not be established when an RSS has visible GSs. In other words, solving SGLs and ILLs planning problems jointly or separately will not change the optimal results of maximizing linking benefits.

Consequently, the loss of optimality from MO-MILP to PMO is whether link planning is considered in flow planning and resource management. In the SGLs and ILLs planning problems of PMO, the consideration of mission importance factors contributes to flow management. So they laid a good foundation for arranging important mission flows in the multi-objective optimization problem. The three optimization problems in PMO are interrelated and jointly contribute to maximizing the data transmission benefits, maximizing the harvested energy, and minimizing transmission wait time. Therefore, PMO has good optimality, and there is not much performance loss compared to MO-MILP.

E. Complexity Analysis

Theorem 3. *The time complexity of the PMO algorithm is approximately upper bounded by $O(\max\{2^{N_g \cdot T_g}, 2^{N_c \cdot T_c}, (F_i \cdot T_g + F_i \cdot T_c + T_c)^3\})$.*

Proof. (a) **Complexity of Steps 2~5 in Algorithm 1 for the SGLs and ILLs planning problems.** The two link planning problems are both ILP problems, which can be solved by the Branch and Bound (B&B) algorithm with exponential time complexity related to the number of integer variables [24]. Since there are $N_g \cdot T_g$ and $N_c \cdot T_c$ integer variables in SGLs and ILLs problems, respectively, the complexity of steps 2~5 is $O(2^{N_g \cdot T_g}) + O(2^{N_c \cdot T_c}) \approx O(\max\{2^{N_g \cdot T_g}, 2^{N_c \cdot T_c}\})$.

(b) **Complexity of Step 6 in Algorithm 1 for the linear weighted multi-objective flow planning and resource management problem.** The LP problem (38) has $F_i \cdot T_g$ and $F_i \cdot T_c$ continuous variables of q_i^g and q_i^c , and T_c continuous variables of E_i^H . It can be solved in polynomial time by the interior algorithm with the complexity of $O((F_i \cdot T_g + F_i \cdot T_c + T_c)^3)$ [25].

Since the PMO algorithm is distributed, the solving program for each RSS can be executed concurrently. Therefore, the total complexity of PMO is upper bounded by $O(\max\{2^{N_g \cdot T_g}, 2^{N_c \cdot T_c}\}) + O((F_i \cdot T_g + F_i \cdot T_c + T_c)^3) \approx O(\max\{2^{N_g \cdot T_g}, 2^{N_c \cdot T_c}, (F_i \cdot T_g + F_i \cdot T_c + T_c)^3\})$. \square

The MO-MILP model has $N_g \cdot T_g + N_c \cdot T_c$ integer decision variables and $F \cdot T_g + F \cdot T_c + T_c$ continuous decision variables. The complexity of the total MO-MILP problem is hard to estimate. We can only know that the integer-related part solved by the B&B algorithm has the worst complexity of $O(2^{N_g \cdot T_g + N_c \cdot T_c})$, which is much larger than the complexity of the PMO algorithm. If further taking the continuous variables into account, the complexity of the total MO-MILP will be even larger. When there are lots of satellites and a long planning horizon, it is a too huge and complex optimization problem to be solved.

The proposed PMO can reduce time complexity by separating the integer programming part from the continuous programming part. As introduced before, we divide the MO-MILP problem into two ILP problems and one LP problem in PMO. The ILP problems can be solved with much fewer integer variables and a much shorter solution time. Taking integer variables as known parameters, the LP problem can also be easily solved. In a word, the proposed PMO can obtain an approximate solution of the MO-MILP model with much less complexity.

VI. SIMULATION AND ANALYSIS

In this section, we first illustrate the settings of the simulation scenario, parameters, and the applied software. Then we simulate and analyze the proposed method in three aspects: 1) the result analysis of a certain RSS, 2) the indicator comprehensive analysis with different data transmission rates, and 3) the solution time and results comparison with other four algorithms under systems with different number of satellites.

A. Simulation Settings

We simulate the SIN with five GSs and three LEO systems consisting of 36, 136, and 500 satellites. The location parameters of GSs are listed in TABLE II. The GSs' locations are relatively concentrated except for the North Pole station. The orbit parameters of satellites in the three LEO systems are listed in TABLE III. The CC satellites are in polar orbits with Walker-Delta configuration and their orbit parameters are referred to the Iridium [26]. The RSSs are in solar synchronous orbits with Walker-Delta configuration and their orbit parameters are referred to the Cosmo-SkyMed [27]. We use the Satellite Tool Kit (STK) software to generate constellations and obtain satellites' time-varying coordinates and lighting information.

Simulation parameters are listed in TABLE IV. The parameters of RSSs are referred to the Cosmo-SkyMed [27], whose satellites are equipped with SAR-2000 Synthetic Aperture Radar. We consider each RSS executes observing missions at the STRIPMAP mode with a duration of 2~6 minutes and 7kW power consumption. Each RSS has a data acquisition rate of 2.4Gbit/s. Each SGL is in X-band with a data downlink rate randomly taken from the interval [0.2, 0.3]Gbit/s. Each ILL is in a laser band with a data transmission rate taken from the set {0.5, 1, 1.5, 2}Gbit/s. We set the planning horizon to be 98 minutes, which is the orbital period of RSSs. Since SAR-2000 has a duty cycle of 20%, each RSS executes 6 observing missions during a period and the total observing duration is less than 18 minutes. Missions' importance factors are evenly selected from the interval [1, 10]. The solar panels of each RSS have 4kW output power. The transmission power consumption of SGL and ILL is set to $P^{Sc}=0.1\text{kW}$ and $P^{Sg}=0.5\text{kW}$, referred to [28]. We set the battery and memory capacity of each RSS to be $E_i^{\max}=32000\text{kJ}$ and $b_i^{\max}=2000\text{Gbit}$ to satisfy the needs of observing missions. According to [22], the time slot duration $\Delta\tau_c$ is set equal to the maximum ILL handover interval, which is 120s. Other parameters, such as the geocentric angle $\xi_i(k, t)$, link distances $d_i^g(k, t)$, and sunlight duration $l_{i,t}$ are calculated by the satellites' and GSs' position coordinates obtained from STK software.

TABLE II
LOCATION INFORMATION OF GSs

	Kashi	Kunming	Sanya	Miyun	North Pole
Latitude (deg)	39.505	25.0273	18.313	40.4514	67.8833
Longitude (deg)	75.929	102.796	109.311	116.859	21.0667
Altitude (km)	1.255	1.955	0.018	0.099	0

TABLE III
ORBIT PARAMETERS OF SATELLITES.

Cases	System-36	System-136	System-500
CC	Walker N/P/F	18/18/1	66/6/1
	Inclination (deg)	86.4	
	Altitude (km)	780	
RSSs	Walker N/P/F	18/18/1	70/10/1
	Inclination (deg)	97.86	
	Altitude (km)	619.6	

TABLE IV
VALUES OF PARAMETERS

Parameters	Values	Parameters	Values
T_g	5880	T_c	49
$\Delta\tau_g$	1s	$\Delta\tau_c$	120s
ν_i^{or}	2.4Gbit/s	$\nu_i^{rg}(k)$	[0.2, 0.3]Gbit/s
$\nu_i^{rc}(j)$	{0.5, 1, 1.5, 2}Gbit/s	ε_{\min}	10deg
$h_i(f)$	[2, 6]min	$\omega_i(f)$	[1, 10]
$b_{i,0}$	0	b_i^{\max}	2000Gbit
$E_{i,0}$	32000kJ	E_i^{\max}	32000kJ
θ	35%	P^H	4kW
P^M	7kW	P^O	0.3kW
P^{Sc}	0.1kW	P^{Sg}	0.5kW

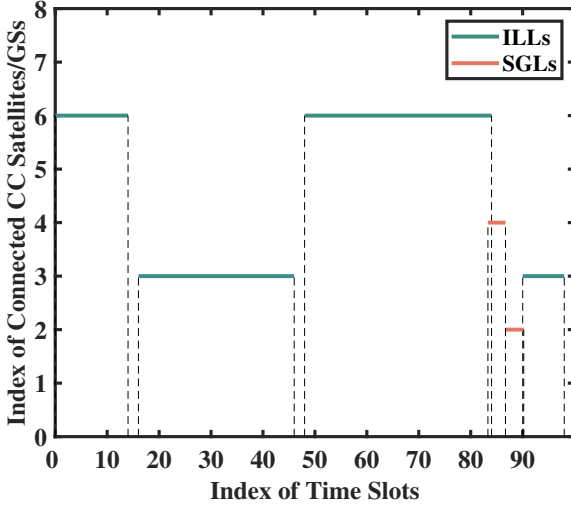


Fig. 4. The linking status of an RSS.

The simulation is executed on Dell 7080MT Optiplex with Intel(R) Core(TM) i7-10700 CPU@ 2.90GHz, 32GB RAM with Windows 11 system, and MATLAB R2022b software. We solve the ILP, LP, and MILP optimization problems mentioned in this paper by solver Gurobi [29] with the modeling tool Yalmip [30].

B. Results of a Certain RSS

The linking status of a certain RSS is shown in Fig. 4. It can be seen that the RSS connects to two GSs and two CC satellites during its orbital period. The SGLs' handover is performed without time interval, while the ILLs' handover is discontinuous since constraints (20)–(21) guarantee necessary handover time for laser capture. Except for the ILLs' handover time, the entire orbital period is covered by communication links so that the RSS can transmit mission data in near real-time. In addition, since we apply the fine-grained time slot division method for SGLs with $\Delta\tau_g$ be 1s, the SGLs can be arranged to their maximum duration in GSs' visible time. Different duration of time slots for ILLs and SGLs also make them overlap shortly so that a seamless transition between ILLs and SGLs can be realized.

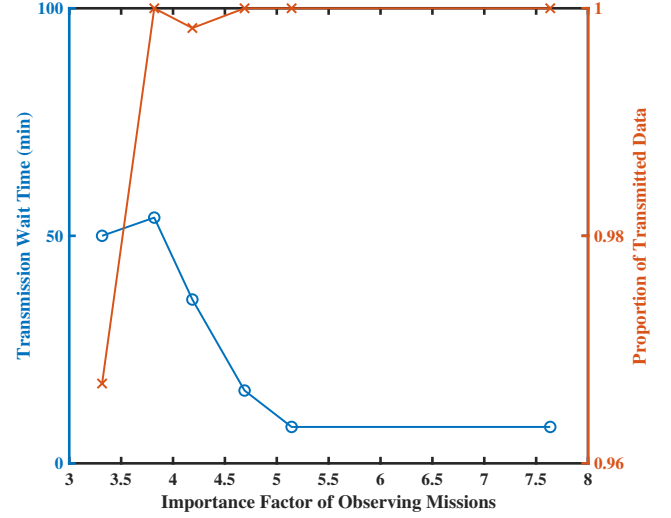


Fig. 5. The relationship between transmission wait time, the proportion of transmitted mission data, and the importance factors of different missions (ILLs' data transmission rate $\nu_i^{rc}(j)=0.5$ Gbit/s).

Fig. 5 shows the relationship between transmission wait time, the proportion of transmitted mission data, and the importance factors of different missions. Since the RSS has 6 missions during the orbital period, there are 6 points on each curve with their importance factors in ascending order. The transmission wait time of each mission is defined as the time difference between the finished time of mission data transmission and the finished time of data acquisition. While for those missions that have not been able to transmit all collected data, the transmission wait time is calculated by $T_c - t_i^e(f)$.

In Fig. 5, the ILLs' data rate are set to 0.5Gbit/s so that the link bandwidth is limited for observation data transmission. We can notice that the transmission wait time is in a downward trend, while the proportion of transmitted data is in an upward trend. This is in line with our expectations since we want important missions can transmit more data as soon as possible. The two curves are not strictly decreasing or increasing, because the data transmission results are also related to the missions' observing time and the remaining resources at that time. Four missions transmitted all data with their proportion being 1, among these missions, three missions' transmission wait time is less than 20 minutes. The other mission needs to wait 54 minutes because of its lower importance factor and the limited link resources. Two missions failed to complete data transmission and waited for the next planning horizon.

To sum up, we verify the planning effectiveness of SGLs and ILLs and show the consideration of missions' importance differences in this subsection.

C. Indicator Analysis with Different Data Transmission Rate

In this subsection, we analyze the simulation results of **System-36**.

Fig. 6 shows the total benefits of this system under different data transmission rates of ILLs. The dotted line represents

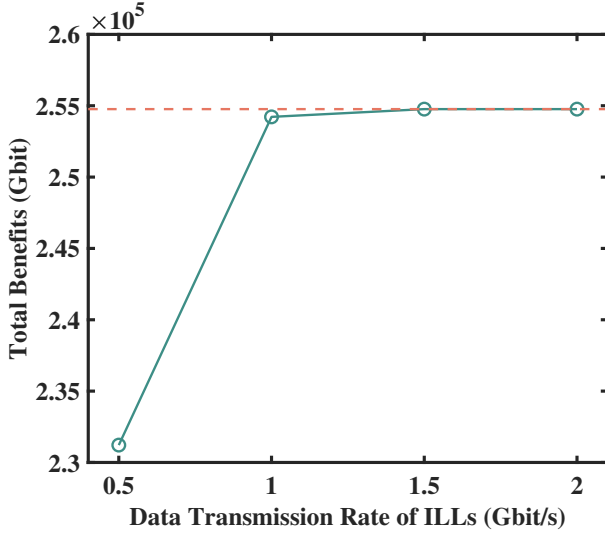


Fig. 6. Total benefits under different data transmission rates of ILLs (in **System-36**).

TABLE V
INDICATORS COMPARISON WITH DIFFERENT DATA TRANSMISSION RATE

	$\nu_i^{rc}(j)$ (Gbit/s)	0.5	1	2
1	Gained benefits proportion	91.33%	99.80%	100%
2	SGLs gained benefits proportion	1.71%	1%	0.3%
3	Average transmission wait time (min)	19.45	7.12	2.54
4	Transmission duration proportion	76.08%	48.87%	29.02%
5	Peak memory usage (Gbit)	1536	1056	308
6	Peak battery usage (kJ)	6400	6381	6309
7	Average energy consumption of ILLs	432.36	255.45	129.10

the total benefits generated from observing missions. With the increase of ILLs' bandwidth, the transmission benefits also increase and gradually approach the observing benefits.

TABLE V shows some indicators comparison with ILLs' data transmission rate be $\{0.5, 1, 2\}$ Gbit/s.

From TABLE V, several conclusions can be obtained:

- From indicators 1 and 2, we can see that SGLs have little contribution in gaining benefits because of their limited visible duration and data transmission rate. Especially as the rate of ILLs increases, the effect of SGLs becomes minimal.
- Indicator 3 shows that when the transmission resources are sufficient, each mission only needs to wait about 2.54 minutes from data acquisition to complete the transmission. This time is far less than the scenario with only SGLs since RSS sometimes needs to wait even more than an orbital period to connect to GSs within a limited area.
- Indicator 4 shows the total transmission duration proportion during an orbital period. As the ILLs' rate increases, the needed transmission duration decreases.
- From indicator 5, we can notice that with a greater data transmission rate, the needed onboard memory decreases sharply. If the observing data can be transmitted as soon as obtained, a small memory is adequate.
- Indicator 6 shows that different data transmission rates

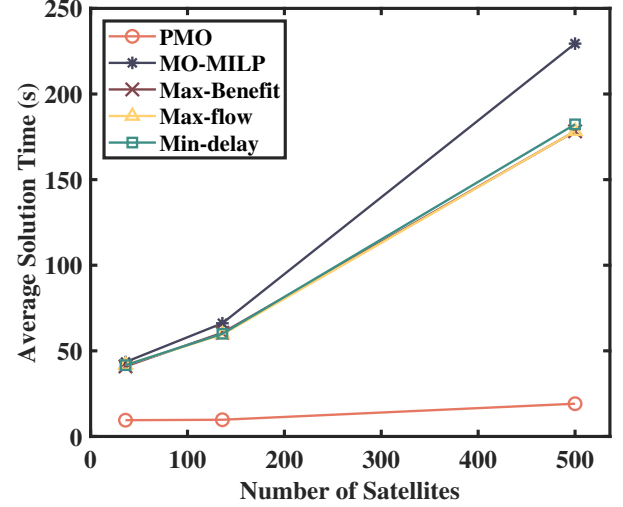


Fig. 7. Average solution time of PMO and other four algorithms under different number of satellites (ILLs' data transmission rate $\nu_i^{rc}(j)=0.5$ Gbit/s).

have little impact on battery usage. This is because the observing mission power of 7kW is much larger than the data transmission power of 0.1kW and 0.5kW. So compared to the energy consumption of SAR, data transmission consumes much less energy.

- Indicator 7 lists ILLs' energy consumption during an orbital period, these values are less than 5% of total energy consumption. From indicators 1, 2, and 7, we can see that ILLs contribute a lot in gaining benefits but consume little energy.

Similar conclusions can also be obtained in **System-136** and **System-500**.

D. Comparison with Other Algorithms

In this subsection, we compare PMO with several other algorithms. The description of these algorithms are as follows:

- MO-MILP: a linear weighted multi-objective model corresponds to (46).
- Max-benefit: an MILP model with the same constraints and variables as in (46), and with $\max y_1$ of (35) be the only objective, which aims to maximize the gained total benefits. A similar model is studied in [19].
- Max-flow: an MILP model with the same constraints and variables as in (46), and with $\max \sum_{f \in \mathcal{F}_i} \{ \sum_{t \in \mathcal{T}^g} q_i^g(f, t) + \sum_{t \in \mathcal{T}^c} q_i^c(f, t) \}$ be the only objective, which aims to maximize the total amount of transmitted data. A similar model is studied in [18], [20].
- Min-delay: an MILP model with the same constraints and variables as in (46), and with $\min \sum_{f \in \mathcal{F}_i} \sum_{t \in \mathcal{T}^c} [(t - t_i^s(f))b_i(f, t)]$ be the only objective, which aims to minimize the delay to GSs/CC of all flows. The delay is defined as the time from data collected to transmitted. Mission importance differences are not considered. A similar model is studied in [21].

TABLE VI
INDICATORS COMPARISON OF ALGORITHMS IN **SYSTEM-136** WITH ILLs' DATA TRANSMISSION RATE $\nu_i^{rc}(j) = 0.5\text{Gbit/s}$

	PMO	MO-MILP	Max-benefit	Max-flow	Min-delay
Total benefits ($\times 10^5\text{Gbit}$)	8.6245	8.6309	8.6309	8.1417	8.1928
Total transmitted data amount ($\times 10^5\text{Gbit}$)	1.4982	1.5	1.5	1.5	1.5
Average end-of-period energy of each RSS ($\times 10^5\text{kJ}$)	3.1910	3.1909	3.1019	3.1020	3.1020
Average transmission wait time of each mission (min)	19.7954	19.7030	35.8218	37.5223	18.8313
Average wait time of top 33% important missions (min)	12	11.9286	31.6143	33.3286	18.3429
Average solution time (s)	9.7544	66.1153	60.5524	59.5857	59.9770

We compare the average solution time of these algorithms under different number of satellites in Fig. 7 with ILLs' data transmission rate be 0.5Gbit/s. It can be seen that the solution time of PMO increases slowly with the number of satellites, while that of the other four algorithms based on MILP increases sharply. MO-MILP has the longest solution time. The results indicate that PMO is more applicable to large-scale constellation systems.

We compare the simulation results of these algorithms in **System-136** with ILLs' data transmission rate be 0.5Gbit/s and list several indicators in TABLE VI. The best solutions for each indicator are marked in bold in this table. The indicators of transmission wait time only consider missions that have transmitted all data.

From this table, several conclusions can be obtained as follows:

- The MO-MILP model can obtain the best results in almost all indicators since it considers benefits, end-of-period energy, and transmission wait time by jointly planning links and managing mission flows. But it has the longest solution time.
- PMO can obtain a great solution very close to MO-MILP with quite a short solution time. The optimality loss of PMO results from separating the links planning problems and the flow management problem, as analyzed in Section V-D. The solution time of MO-MILP is almost 7 times of PMO.
- Max-benefit algorithm can not obtain larger benefits than MO-MILP, it indicates that the linear weighting method described in **Theorem 2** can guarantee the primary goal of benefits maximization.
- Max-flow algorithm can not obtain more transmitted data amount than MO-MILP and Max-benefit, and has less benefits. It indicates that MO-MILP and Max-benefit can achieve the upper limit of transmission capacity, and the consideration of mission importance differences is effective for transmitting important data.
- Min-delay algorithm can obtain the minimum average transmission wait time, but the wait time of important missions have not much differences. Besides, the gained benefits are significantly inferior to the optimal value.
- Focus on the indicator of end-of-period energy, PMO and MO-MILP have about 9000kJ energy more than the other algorithms at the end of this period. It indicates that the consideration of maximizing the onboard energy in (36) is necessary for the long-term stable operation of RSSs.

- Focus on the two indicators of transmission wait time, PMO and MO-MILP can obtain an average transmission wait time not differ much from the optimal value obtained by Min-delay. Meanwhile, PMO and MO-MILP can obtain the shortest wait time for important missions. It indicates that the minimization of mission-weighted stored data volume in (37) can effectively reduce transmission wait time and is especially beneficial for important missions.

To sum up, PMO can jointly optimize benefits, end-of-period energy and transmission wait time with the consideration of mission importance differences in a short solution time.

VII. CONCLUSION

In this paper, we propose a link planning and flow management method from the perspective of each RSS in SIN based on a time-expanded graph. The RSS is considered to transmit data to GSs and CC through SGLs and ILLs to achieve optimal data transmission. For this purpose, we propose a PMO algorithm composed of two ILP problems and one LP optimization problem. The two ILP problems can achieve SGLs and ILLs optimal planning, and the LP problem can jointly achieve transmission benefits maximization, end-of-period energy maximization, and mission-weighted transmission wait time minimization. An MO-MILP model is also formulated for comparison. We simulate the proposed models and algorithms in the SIN with five GSs and three LEO systems consisting of 36, 136, 500 satellites. Simulation results show that the consideration of missions' importance factor can make important missions' data be transmitted with a short wait time and larger volume. Compared to only transmitted data by SGLs in the traditional system, ILLs contribute a lot in gaining benefits and reducing transmission wait time with little energy consumption. Compared with other algorithms, the proposed PMO can obtain a great solution of multiple objectives and has good solving performance in large-scale constellation systems.

In the future, we will add observation planning to the proposed model and consider the missions in a more realistic scenario, such as the location of observing targets and the attitude transition time between different missions.

REFERENCES

- [1] H. Lu, Y. Gui, X. Jiang, F. Wu, and C. W. Chen, "Compressed robust transmission for remote sensing services in space information networks," *IEEE Wireless Communications*, vol. 26, no. 2, pp. 46–54, Apr. 2019.

- [2] L. Zhao, Q. Zhang, Y. Li, Y. Qi, X. Yuan, J. Liu, and H. Li, "China's gaofen-3 satellite system and its application and prospect," *IEEE Journal of Selected Topics in Applied Earth Observations and Remote Sensing*, vol. 14, pp. 11 019–11 028, 2021.
- [3] "Oneweb: Space is the future," OneWeb, 2023. [Online]. Available: <https://oneweb.net/>
- [4] "Starlink: World's most advanced broadband satellite internet," SpaceX, 2023. [Online]. Available: <https://www.starlink.com/technology>
- [5] "Telesat lightspeed™: Affordable, quality internet everywhere," Telesat, 2023. [Online]. Available: <https://www.telesat.com/leo-satellites/>
- [6] M. Toyoshima, "Recent trends in space laser communications for small satellites and constellations," *Journal of Lightwave Technology*, vol. 39, no. 3, pp. 693–699, 2021.
- [7] H. Al-Hraishawi, M. Minardi, H. Chougrani, O. Kodheli, J. F. M. Montoya, and S. Chatzinotas, "Multi-layer space information networks: Access design and softwarization," *IEEE Access*, vol. 9, pp. 158 587–158 598, Nov. 2021.
- [8] X. Zhang, L. Zhu, T. Li, Y. Xia, and W. Zhuang, "Multiple-user transmission in space information networks: Architecture and key techniques," *IEEE Wireless Communications*, vol. 26, no. 2, pp. 17–23, Apr. 2019.
- [9] M. Y. Abdelsadek, A. U. Chaudhry, T. Darwish, E. Erdogan, G. Karabulut-Kurt, P. G. Madoery, O. Ben Yahia, and H. Yanikomeroglu, "Future space networks: Toward the next giant leap for humankind," *IEEE Transactions on Communications*, vol. 71, no. 2, pp. 949–1007, Feb. 2023.
- [10] S. Ji, M. Sheng, D. Zhou, W. Bai, Q. Cao, and J. Li, "Flexible and distributed mobility management for integrated terrestrial-satellite networks: Challenges, architectures, and approaches," *IEEE Network*, vol. 35, no. 4, pp. 73–81, Aug. 2021.
- [11] J. Huang, Y. Su, L. Huang, W. Liu, and F. Wang, "An optimized snapshot division strategy for satellite network in gnss," *IEEE Communications Letters*, vol. 20, no. 12, pp. 2406–2409, Dec. 2016.
- [12] J. Yang, K. Sun, H. He, X. Jiang, and S. Chen, "Dynamic virtual topology aided networking and routing for aeronautical ad-hoc networks," *IEEE Transactions on Communications*, vol. 70, no. 7, pp. 4702–4716, Jul. 2022.
- [13] Z. Hou, X. Yi, Y. Zhang, Y. Kuang, and Y. Zhao, "Satellite-ground link planning for LEO satellite navigation augmentation networks," *IEEE Access*, vol. 7, pp. 98 715–98 724, Jul. 2019.
- [14] Y. Li, Y. Wang, Q. Zhang, and Z. Yang, "Tcds: A time-relevant graph based topology control in triple-layer satellite networks," *IEEE Wireless Communications Letters*, vol. 9, no. 3, pp. 424–428, Mar. 2020.
- [15] Y. Huang, B. Feng, P. Dong, A. Tian, and S. Yu, "A multi-objective based inter-layer link allocation scheme for MEO/LEO satellite networks," in *2022 IEEE Wireless Communications and Networking Conference (WCNC)*, Apr. 2022, pp. 1301–1306.
- [16] K. Shi, X. Zhang, S. Zhang, and H. Li, "Time-expanded graph based energy-efficient delay-bounded multicast over satellite networks," *IEEE Transactions on Vehicular Technology*, vol. 69, no. 9, pp. 10 380–10 384, Sep. 2020.
- [17] P. Wang, X. Zhang, S. Zhang, H. Li, and T. Zhang, "Time-expanded graph-based resource allocation over the satellite networks," *IEEE Wireless Communications Letters*, vol. 8, no. 2, pp. 360–363, Apr. 2019.
- [18] W. Liu, L. Zhu, H. Yang, H. Li, J. Li, and A. M.-C. So, "Maximum flow routing strategy with dynamic link allocation for space information networks under transceiver constraints," *IEEE Transactions on Vehicular Technology*, vol. 71, no. 9, pp. 9993–10 000, Sep. 2022.
- [19] D. Zhou, M. Sheng, X. Wang, C. Xu, R. Liu, and J. Li, "Mission aware contact plan design in resource-limited small satellite networks," *IEEE Transactions on Communications*, vol. 65, no. 6, pp. 2451–2466, Jun. 2017.
- [20] Z. Yan, G. Gu, K. Zhao, Q. Wang, G. Li, X. Nie, H. Yang, and S. Du, "Integer linear programming based topology design for GNSSs with inter-satellite links," *IEEE Wireless Communications Letters*, vol. 10, no. 2, pp. 286–290, Feb. 2021.
- [21] Z. Yan, K. Zhao, W. Li, C. Kang, J. Zheng, H. Yang, and S. Du, "Topology design for GNSSs under polling mechanism considering both inter-satellite links and ground-satellite links," *IEEE Transactions on Vehicular Technology*, vol. 71, no. 2, pp. 2084–2097, Feb. 2022.
- [22] N. Guo, L. Liu, and X. Zhong, "Task-aware distributed inter-layer topology optimization method in resource-limited LEO-LEO satellite networks," *IEEE Transactions on Wireless Communications*, pp. 1–1, Sep. 2023.
- [23] K. Deb, K. Sindhya, and J. Hakanen, "Multi-objective optimization," in *Decision sciences*. CRC Press, 2016, pp. 161–200.
- [24] D. R. Morrison, S. H. Jacobson, J. J. Sauppe, and E. C. Sewell, "Branch-and-bound algorithms: A survey of recent advances in searching, branching, and pruning," *Discrete Optimization*, vol. 19, pp. 79–102, Feb. 2016.
- [25] F. A. Potra and S. J. Wright, "Interior-point methods," *Journal of Computational and Applied Mathematics*, vol. 124, no. 1, pp. 281–302, Dec. 2000.
- [26] "Iridium: Perfectly in sync, while traveling more than 30,000 kilometers per hour," Iridium Communications Inc, 2023. [Online]. Available: <https://www.iridium.com/network/>
- [27] "Cosmo-skymed," eoPortal, 2023. [Online]. Available: <https://www.eoportal.org/satellite-missions/cosmo-skymed#references>
- [28] W. Yan, C. Peiyong, S. Yiwei, F. U. Sen, and N. Junpo, "Progress on the development and trend of overseas space laser communication technology (in chinese)," *Flight Control & Detection*, vol. 2, no. 1, pp. 8–16, Jan. 2019.
- [29] "Gurobi optimization, solve complex problems, fast," GUROBI OPTIMIZATION, LLC., 2023. [Online]. Available: <https://www.gurobi.com>
- [30] J. Löfberg, "Yalmip," Jekyll & Minimal Mistakes, 2023. [Online]. Available: <https://yalmip.github.io/>